Neuron, Vol. 19, 77–89, July, 1997, Copyright ©1997 by Cell Press

Axon Patterning Requires *D*N-cadherin, a Novel Neuronal Adhesion Receptor, in the Drosophila Embryonic CNS

Youichi Iwai,* Tadao Usui,* Shinji Hirano,*‡ Ruth Steward,† Masatoshi Takeichi,* and Tadashi Uemura*

*Department of Biophysics
Faculty of Science
Kyoto University
Kitashirakawa
Sakyo-ku
Kyoto 606–01
Japan

†Department of Molecular Biology
Rutgers University
Waksman Institute
Piscataway, New Jersey 08855–0759

Summary

We identified *D*N-cadherin, a novel Drosophila cadherin that is expressed in axons and in the mesoderm. Although *D*N-cadherin has diverged from vertebrate classic cadherins in terms of its extracellular structure, it still can form a complex with catenins and induce cell aggregation, as do the vertebrate molecules. Loss-of-function mutations of the gene resulted in either embryonic lethality or uncoordinated locomotion of adults. In the central nervous system of null mutant embryos, subsets of ipsilateral axons displayed a variety of aberrant trajectories including failure of position shifts, defective bundling, and errors in directional migration of growth cones. These results suggest that processes of axon patterning critically depend on *D*N-cadherin-mediated axon–axon interactions.

Introduction

Directed outgrowth of axons is fundamental to establish the initial formation of neuronal connections. Axons are guided either by contact-mediated mechanisms or by diffusible substances. In the contact-mediated mechanisms, guidance signals can be transmitted, for example, through direct contacts between the growth cone and the surface of guidepost cells or preexisting pioneer axons (reviewed by Keynes and Cook, 1995; Goodman 1996; Tessier-Lavigne and Goodman, 1996). Numerous cell surface molecules have been postulated or suggested to play roles in axonal guidance or outgrowth. For example, several molecules, which belong to the immunoglobulin (Ig) superfamily, have been shown to be critical for axon guidance. The homophilic adhesion molecule fasciclin II, related to N-CAM, is essential for selective axon fasciculation (Grenningloh et al., 1991; Lin et al., 1994). Ig-like domains have been found in other guidance molecules, including Irregular chiasm C-roughest (Schneider et al., 1995) and a potential netrin receptor, Frazzled (Kolodziej et al., 1996), which is homologous to DCC and UNC-40 (Chan et al., 1996; Keino-Masu et al., 1996).

Adhesion receptors of the cadherin family (reviewed by Ranscht, 1994; Redies and Takeichi, 1996) have also been implicated in axon outgrowth as well as in other aspects of neural morphogenesis, including segmental subdivision of the brain and synaptogenesis (for examples, Matsunaga et al., 1988; Bixby and Zhang, 1990; Matsunami and Takeichi, 1995; Fannon and Colman, 1996; Uchida et al., 1996; reviewed by Doherty and Walsh, 1996; Redies and Takeichi, 1996). In these studies, however, most evidence for the role of cadherins was based on in vitro observations. Recently, cadherin function in neurite outgrowth was investigated in vivo by expressing a dominant negative form of N-cadherin in the retina of Xenopus embryos (Riehl et al., 1996). Expression of this mutant molecule severely impaired axon and dendrite outgrowth in retinal ganglion cells. For further exploration of the in vivo roles of cadherin in axon patterning, genetic ablation of any cadherin genes in the whole animal is essential. To this end, Drosophila melanogaster provides an ideal model system because of the anatomical simplicity of its nervous system (Goodman and Doe, 1993; Jan and Jan, 1993) and advanced molecular genetical technology (for example, see O'Kane and Gehring, 1987; Brand and Perrimon, 1993; Spradling et al., 1995).

The cadherin superfamily consists of integral membrane or membrane-anchored proteins that are defined by the presence of unique motifs in the extracellular region. This superfamily can be subdivided into two subfamilies: the classic and nonclassic types (reviewed by Takeichi, 1991, 1995; Huber et al., 1996). The classic-type molecules are simply called cadherins, and they possess Ca^{2+}-dependent cell–cell adhesion activity. The intracellular domains of all vertebrate classic cadherins are structurally highly conserved, with which two classes of cytoplasmic molecules, α- and β-catenins, interact (McCrea et al., 1991; Nagafuchi et al., 1991; Hirano et al., 1992). This molecular assembly is essential for the cadherin to exert its cell–cell adhesion activity (Hirano et al., 1992; Kawanishi et al., 1994; Oyama et al., 1995).

*D*E-cadherin was the first classic-type cadherin to be isolated from the invertebrates, and was shown to associate with the Drosophila catenin homologs *D*α-catenin and Armadillo (β-catenin) (Oda et al., 1994; Cox et al., 1996; Pai et al., 1996). *D*E-cadherin is predominantly expressed by epithelial tissues in embryos (Oda et al., 1994; Tepass et al., 1996). Analyses of the *D*E-cadherin zygotic mutant *shotgun* (*shg*) showed that *D*E-cadherin is critically required for dynamic epithelial rearrangements during embryogenesis (Tanaka-Matakatsu et al., 1996; Tepass et al., 1996; Uemura et al., 1996). Two other molecules of the Drosophila cadherin superfamily were reported: a tumor suppressor, Fat (Mahoney et al., 1991), and Dachsous (Clark et al., 1995). None of these Drosophila molecules are primarily expressed in the nervous system. *D*E-cadherin is expressed in the

‡Present address: DVRC 309, Doheny Eye Institute, 1355 San Pablo Street, Los Angeles, California 90033.

embryonic nervous system, but its expression is limited to midline glial cells of the central nervous system (CNS) and also to adherens junctions between sensory dendrites and their accessory cells in the periphery (Oda et al., 1994; H. Oda and T. U., unpublished data).

Loss of zygotically expressed *D*E-cadherin was shown to result in a great reduction of catenins in the epithelia; however, the axons remained enriched in catenins (Tepass et al., 1996; Uemura et al., 1996). This was strongly indicative of the presence of distinct cadherins in axonal membranes. We searched for such cadherins and identified *D*N-cadherin as the major axonal cadherin. Then we isolated strong and weak loss-of-function mutations of the *D*N-cadherin gene and studied their phenotypes, focusing on formation of several distinct axon fascicles in strong embryonic lethal alleles. Our investigation revealed various defects in axon fascicle formation in the mutants, providing novel genetic evidence at the whole-animal level of roles for the cadherin family in axon patterning.

Results

Cloning and Sequence of *D*N-cadherin cDNA

To identify novel cadherin genes, we first designed degenerate primers complementary to intracellular sequences that are highly conserved between vertebrate classic cadherins and *D*E-cadherin. However, we could amplify no novel Drosophila cadherin gene by this means. To collect information about sequences conserved among insect cadherins, we partially determined structures of cDNA clones of two Bombyx cadherins; those data were then incorporated to refine our primer design (see details in Experimental Procedures). By using one pair of new primers, we successfully isolated cDNA of an intracellular portion of a novel Drosophila cadherin. In addition to these approaches, we performed another polymerase chain reaction (PCR) with primers that match consensus sequences of the extracellular cadherin repeat. A combination of both strategies led us to isolate cDNA clones that covered the entire open reading frame of the novel gene. Subsequent studies of its expression pattern and mutants suggested that this gene encodes a major cadherin molecule expressed by neurons. Therefore, we designated this molecule as *D*N-cadherin (Drosophila neuronal cadherin).

The predicted translational product had 3097 amino acids. This enormous size is primarily due to the presence of 15 cadherin repeats in the extracellular region (CR1–CR15, Figures 1A and 1B), presenting a contrast to the 4 repeats in all vertebrate classic cadherins and the 6 repeats in *D*E-cadherin. Both Drosophila cadherins had insertions of similar sequences between the last CR and the membrane-spanning segment. The *D*N-cadherin insert contained a series of subdomains, Fcc box (fly classic cadherin box), a cysteine-rich segment (C-rich 1), a laminin A globular domain (LmA-G), and another cysteine-rich segment (C-rich 2). The Fcc

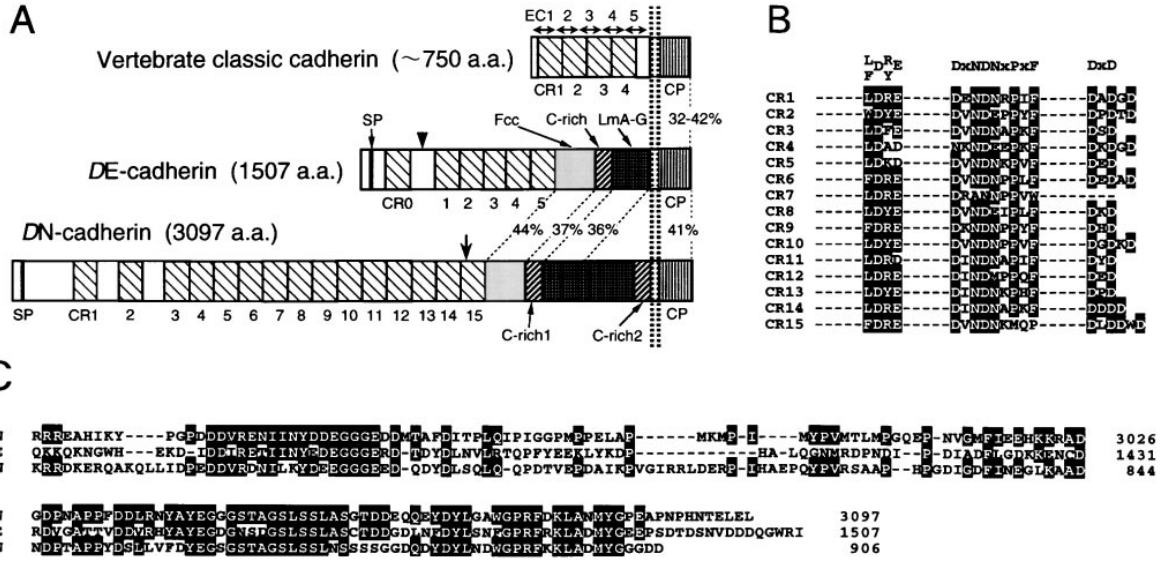

Figure 1. Predicted Primary Structure of *D*N-cadherin

(A) Schematic representations of the vertebrate classic cadherin and Drosophila cadherins. *D*N-cadherin contains 15 cadherin repeats (CR1–15), Fcc box (fly classic cadherin box), two cysteine-rich domains (C-rich1 and C-rich2), a laminin A globular domain (LmA-G), a membrane-spanning segment, and a cytoplasmic domain (CP). Bars close to the amino termini show signal peptides (SP). Indicated are percent amino acid identities between individual subdomains. Note that the drawn vertebrate molecule represents the mature form, whereas *D*E- and *D*N-cadherins are the entire translational products. CR0 of *D*E-cadherin was speculated to be cleaved off at the site indicated by the triangle (Oda et al., 1994). In contrast, it is difficult to predict the amino terminus of the mature form of *D*N-cadherin. A hypothetical internal cleavage site is indicated by the thick arrow, which would produce the N-terminal 200 kDa and the C-terminal 120 kDa fragments (see Figure 2A). The definition of CR and another definition of structural reiteration, EC, are described by Takeichi (1991, 1995).

(B) Cadherin repeats of *D*N-cadherin are aligned to highlight conserved residues (black boxes). They fit very well to consensus sequences that are characteristic of the cadherin repeat (top); Xs represent residues that are not strictly fixed in the cadherin superfamily.

(C) Sequence similarity of intracellular domains of *D*N-caderin, *D*E-cadherin, and mouse N-cadherin (mN). Identical residues between *D*N-cadherin and the other proteins are shown in black boxes. Broken lines indicate gaps in the sequences to allow optimal alignment. Numbers denote positions of amino acid residues.

box, comprising 170 amino acids, was defined as such because database searches with its sequences identified only the comparable region of *D*E-cadherin as a relative. The whole *D*N-cadherin LmA-G displayed 25% sequence identity to mouse laminin A (Sasaki et al., 1988) and to the presynaptic transmembrane protein neurexin (Ushkaryov et al., 1992).

In contrast to the extracellular region, the *D*N-cadherin cytoplasmic domain was much more similar to those domains of *D*E-cadherin and vertebrate classic cadherins with respect to both size and sequence. The intracellular domains of the two Drosophila cadherins and mouse N-cadherin ranged between 157 and 160 amino acids in length, and had 37%–46% sequence identity in any combination among them (Figure 1C). Nevertheless, the degree of the sequence conservation between the two Drosophila cadherins (41% identity) was lower than the 63% identity between N- and E-cadherin in the same vertebrate species, for example, mice (Nagafuchi et al., 1987; Miyatani et al., 1989).

Characterization of *D*N-cadherin as a Classic Cadherin Type of Adhesion Molecule

We raised antibodies to the extracellular domain and to the cytoplasmic region of *D*N-cadherin and designated them as DN-Ex and DN-In, respectively. These antibodies specifically recognized multiple *D*N-cadherin polypeptides in lysates of whole embryos or S2 cells transfected with a *D*N-cadherin cDNA construct (Figure 2A). Both DN-Ex and DN-In recognized a pair of bands of roughly 300 kDa (arrow and triangle in Figure 2A), of which the upper band was always faint. When *D*α-catenin was immunoprecipitated, the smaller band was easily detected in the precipitated fraction, but the other was not. Hence, we assume that the larger band is the precursor and that the smaller one represents the mature form generated by proteolytic digestion of the other. This assumption was corroborated by isolation of a mutation that accumulated the larger form, as described later.

Besides the above high molecular weight forms, DN-Ex detected a major 200 kDa molecule, and DN-In labeled an intense 120 kDa band. We can explain the production of these two fragments by postulating that the mature form is cleaved into an N-terminal 200 kDa and a C-terminal 120 kDa fragment at around the site indicated by the arrow in Figure 1A. In this hypothesis, the 200 kDa form is derived only from the extracellular domain, which was supported by our observation that the 200 kDa band was still present in a *D*N-cadherin mutant strain that had a nonsense mutation at a proximal position in the extracellular domain (explained later in Figure 4), while the 120 kDa was missing. Upon immunoprecipitation of *D*α-catenin, not only the mature form and the 120 kDa fragment but also the 200 kDa form were coprecipitated with *D*α-catenin. Furthermore, the 200 kDa molecule was detected in S2 transfectants even after extensive washing, suggesting that it is not soluble but associated with cell surfaces. The 200 kDa molecule may bind to an intact *D*N-cadherin, forming a strand dimer whose presence was predicted by three-dimensional analyses of N- and E-cadherins (Shapiro et al., 1995; Nagar et al., 1996). Further characterization of the 200 kDa and 120 kDa bands remains to be done.

Immunoprecipitation of *D*N-cadherin showed that it binds not only to *D*α-catenin but also to β-catenin/Armadillo (Arm) (Figure 2B). Alternative splicing generates two Arm isoforms: the 105 kDa ubiquitous form and the 82 kDa neural form (Loureiro and Peifer, personal communication). *D*N-cadherin associated predominantly

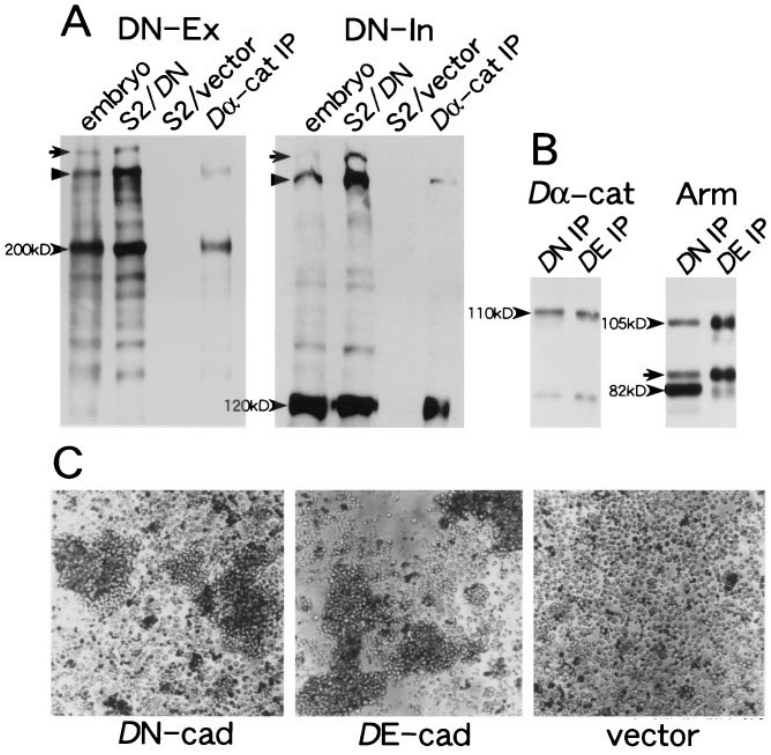

Figure 2. Detection of *D*N-cadherin Polypeptides and Complex Formation with Catenins

(A) Western analyses with antibodies to the extracellular (DN-Ex, left) and intracellular (DN-In, right) domains. *D*N-cadherin polypeptides were detected in extracts of late embryos (embryo) and of S2 cells transfected with a cDNA construct (S2/DN). S2 cells did not produce *D*N-cadherin endogenously (S2/vector). Mobilities of the precursor (arrow) and the mature form (triangle) are indicated. The mature form, 200 kDa, and 120 kDa molecules coimmunoprecipitated with *D*α-catenin (*D*α-cat IP).

(B) *D*N- or *D*E-cadherin was immunoprecipitated from embryonic extracts (*D*N IP or *D*E IP), and the precipitated materials were probed with an antibody to either *D*α-catenin (left) or Armadillo (right). The 82 kDa Arm was a major form that binds to *D*N-cadherin, whereas it was a minor component in the *D*E-cadherin-catenin complex. An arrow points to a degradation product of the 105 kDa Arm.

(C) Both Drosophila cadherins have the ability to induce cell aggregate formation. *D*N-cadherin (left) or *D*E-cadherin (middle) was expressed under a methallothionein promoter in S2 cells. S2 cells exhibited an only very weak self-aggregation property when transfected with the vector (right).

with the 82 kDa Arm, whereas *D*E-cadherin preferentially bound to the 105 kDa isoform. Transfection of Drosophila S2 cells with *D*N-cadherin cDNA induced them to form aggregate (Figure 2C). The activity of *D*N-cadherin was comparable to that of *D*E-cadherin, as the aggregate formation was detectable within 5 min once our assay was started. All of these findings suggest that *D*N-cadherin is functionally homologous to vertebrate classic cadherins, although it has unique features in its extracellular structure.

DN-cadherin Expression in Embryonic Mesoderm and Nervous System

*D*N-cadherin expression was analyzed at both mRNA and protein levels. Its mRNA signals were first seen within nuclei of presumptive mesodermal cells prior to gastrulation at stage 5 (Figures 3A–3C). mRNA transport to the cytoplasm started at around stage 6–7, and the messengers became distributed throughout the cytoplasm by stage 8 (Figure 3D). *D*N-cadherin protein first appeared at intercellular contacts in the mesoderm at stage 9, and then the protein was detected at boundaries of mesodermally derived cells including myoblasts (Figure 3E) and myotubes (Figure 3F); however, it was not found in cardiac cells that initiate transcription of the *D*E-cadherin gene at stage 13 (Tepass et al., 1996; H. Oda and T. U., unpublished data). *D*N-cadherin also appeared in developing neural cells, presumably at their postmitotic stage, and subsequently its protein was accumulated in axons in the entire CNS (Figures 3E and 3F). At the subcellular level, neuronal processes including growth cones were labeled (Figure 3G). In third instar larvae, *D*N-cadherin was expressed in CNS neuropil, photoreceptor axons, and precursors of adult muscles (data not shown). It is noteworthy that gastrulation and neurulation were shown to coincide with a switch of cadherin expression from *D*E- to *D*N-cadherin (Oda et al., 1994; Tepass et al., 1996; H. Oda and T. U., unpublished data).

Whether glial cells express *D*N-cadherin was difficult to address in the wild-type CNS, as they represent only 10% of the total CNS cells (Figure 3H). As an alternative approach, we investigated embryos in which most neurons were transformed into glial cells by ectopic expression of *glial cell missing* (Hosoya et al., 1995; Jones et al., 1995). Under this genetic condition, *D*N-cadherin-expressing cells were negative for the glial marker REPO (Campbell et al., 1994; Xiong et al., 1994; Halter et al., 1995) (Figure 3I) but positive for neuronal markers (data not shown). Therefore, we assume that glial cells do not express *D*N-cadherin in the wild-type situation either.

*D*N-cadherin seems to be the major cadherin that assembles catenins in axons. This view is based on the following observation: As described below, we isolated mutants that produced only a small amount of *D*N-cadherin protein. *D*α-catenin expression was compared between these mutant and wild-type embryos. Intense *D*α-catenin signals were detected in the wild-type axon tract (Oda et al., 1993; Figure 3J), whereas the axonal expression was greatly down-regulated in the mutants, although neuronal cell bodies retained a low level of *D*α-catenin signals (Figure 3K). On the other hand, *D*α-catenin was normally present in midline glial cells and epithelia that synthesize *D*E-cadherin, even in these mutants. Consistently, Western analysis revealed that the level of the 82 kDa neural Arm, as opposed to that of the 105 kDa ubiquitous form, was preferentially reduced in the mutants (Figure 4C). This result provided an exact contrast to the preferential reduction of the 105 kDa ubiquitous form in the *D*E-cadherin mutant (Uemura et al., 1996). Previous studies of cell lines show that catenins are unstable in the absence of cadherins (Nagafuchi et al., 1991, 1994); thus, our results strongly suggest that most if not all axonal catenins associate with *D*N-cadherin in the wild type.

*D*N-cadherin Is Encoded by *l(2)36Da*

We cytologically assigned the *D*N-cadherin gene to bands 36C/D of the second chromosome. This region was previously saturated for loci essential for viability or female fertility (Steward and Nüsslein-Volhard, 1986). *Df(2L)TW119* (*Df*) was the shortest chromosomal deletion that uncovers the *D*N-cadherin gene. We further narrowed down this deficiency and placed the gene in the interval where only *l(2)36Da* was located. The following results led us to conclude that *l(2)36Da* encodes *D*N-cadherin: First, we found that all of the previously isolated six *l(2)36Da* alleles exhibited abnormal staining patterns for *D*N-cadherin (Figure 4A). In embryos homozygous for five individual alleles, numbered M6, M19, M23, M33, and F15, immunoreactivity was greatly reduced or below the level of our detection. In the remaining one allele $l(2)36Da^{M12}$, *D*N-cadherin molecules were mislocalized; those mutant embryos gave perinuclear staining, and their axons were almost devoid of the signals. Second, in two alleles examined, $l(2)36Da^{M19}$ and $l(2)36Da^{M12}$, we identified a nonsense and a missense mutation, respectively, in the *D*N-cadherin gene (Figure 4B). Finally, CNS phenotypes in the *l(2)36Da* mutants could be rescued by *D*N-cadherin cDNA expression (Figure 4A, described later).

Of the five alleles that afforded weak staining for *D*N-cadherin, $l(2)36Da^{M19}$ and $l(2)36Da^{M23}$ gave the most penetrant phenotypes, and the former was chosen for further studies. The nearly protein-null condition in $l(2)36Da^{M19}$ was confirmed by Western blot analysis (Figure 4C). The $l(2)36Da^{M19}$ homozygous embryos produced a trace of the 200 kDa fragment, but neither the mature form nor the 120 kDa fragment was detectable. This result is consistent with the nonsense mutation that caused truncation at a proximal position of the extracellular domain (Figure 4B). Furthermore, $l(2)36Da^{M19}/Df$ embryos and *Df* homozygotes showed similar severity in axonal defects (data not shown). Therefore, $l(2)36Da^{M19}$ appeared to be a complete loss-of-function mutant. The $l(2)36Da^{M19}/Df$ embryos failed to hatch. $l(2)36Da^{M12}$ was a hypomorphic mutation, as $l(2)36Da^{M12}/Df$ and $l(2)36Da^{M12}/l(2)36Da^{M19}$ mutant animals survived to the adult stage. Notably, these mutant adults exhibited strongly uncoordinated or reduced locomotion. The $l(2)36Da^{M12}$ mutation seems to affect protein maturation, as this mutant contained more precursors than the mature form, which is the opposite of the case for the wild type (data not shown). Probably because of less susceptibility to the proteolytic maturation, the mutant polypeptides were not properly sorted out through the secretory pathway, and neither were they transported into axons (Figure 4A; Hammond and Helenius, 1994).

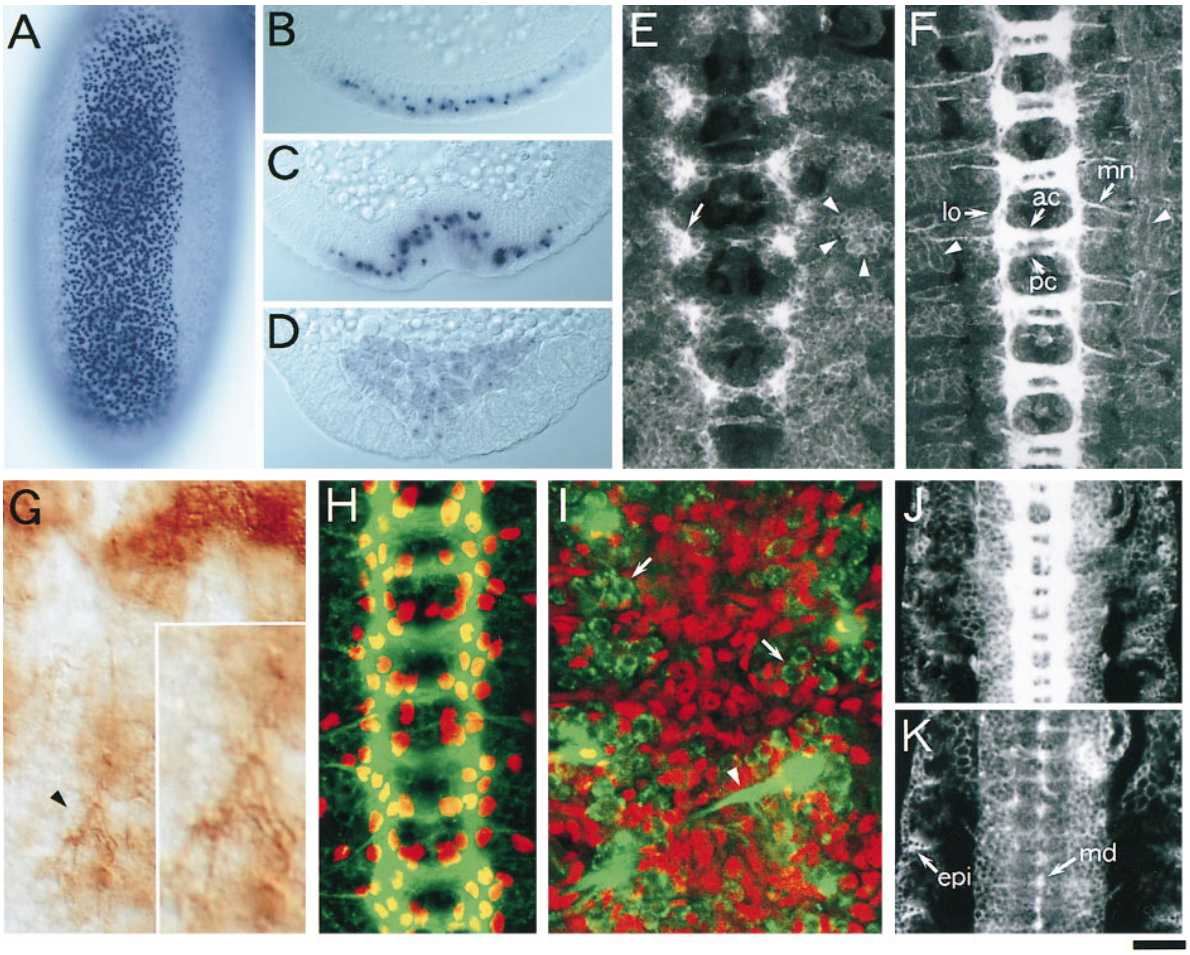

Figure 3. Expression of *D*N-cadherin in Mesoderm and Neurons

(A–D) In situ hybridization of embryos with a *D*N-cadherin RNA probe.

(A) A ventral view of a cellular blastoderm embryo. mRNA synthesis is initiated in the presumptive mesoderm.

(B–D) Cross sections. At the cellular blastoderm stage ([B], stage 5) and during the early phase of gastrulation ([C], stage 6), strong signals are localized within the nuclei.

(D) At stage 8 when the invaginated mesoderm disperses, mRNA is distributed also in the cytoplasm.

(E and F) Ventral views of stage 12 (E) and stage 14 (F) embryos stained with *D*N-cadherin antibody DN-Ex. Arrowheads mark myoblasts (E) and muscle fibers (F). In the developing CNS, intensely labeled are outgrowing axons (arrow) in (E), and anterior commissures (ac), posterior commissures (pc), longitudinal connectives (lo), and motor nerves (mn) in (F).

(G) CNS of late stage 12 embryo stained with DN-Ex and DN-In. The arrowhead marks a growth cone, and its magnified view is shown in an inset.

(H and I) Double labeling with DN-Ex (green) and a glial marker REPO (red) of stage 15 embryos. (H) Wild-type embryo.

(I) An embryo in which *glial cell missing* is ectopically expressed, which causes transformation of most neurons into glia. Consequently, the ladder-like axon tract is never formed and only residual axon bundles are seen (arrowhead). The overproduced glial cells do not express *D*N-cadherin, and nuclei of *D*N-cadherin-positive cells are not labeled by the anti-REPO antibody (arrows).

(J and K) *D*α-catenin localization in the wild type (J) and in a *l(2)36Da*^{M19}*/Df(2L)TW119* mutant (K) at stage 16. The *D*α-catenin expression level is greatly reduced in the ladder-like axon scaffold in the mutant. In contrast, *D*α-catenin is present normally in mutant tissues that express *D*E-cadherin: for example, CNS midline (md) and epidermis (epi). Image acquisition and processing parameters were identical for (J) and (K). Anterior is toward the top except for (B–D) and (G). In (G), anterior is toward the left. The scale bars indicate 50 μm (A), 20 μm (B–D), 18 μm ([E] and [F]), 6 μm (G), 10 μm ([H] and [I]), and 20 μm ([J] and [K]).

Fasciclin II-Expressing Tracts are Deformed in the Mutants

We investigated developing nervous systems of *l(2)36Da*^{M19}*/Df* embryos by use of markers to label all or restricted populations of neurons. Overall neuronal staining allowed us to detect subtle phenotypic differences; the mutant axon scaffold was slightly less compact in the transverse direction, and intersegmental longitudinal connectives were thinner than the normal ones (Figures 6E and 6F). No adhesive defect was apparent in the cell body regions. However, significant phenotypes were observed when we focused on the subsets of neurons expressing either Fasciclin II (Fas II; Grenningloh et al., 1991) or *apterous* (Lundgren et al., 1995).

Anti-Fas II antibody labels four neurons that pioneer the first two longitudinal axon pathways, vMP2 and MP1 (Goodman and Doe, 1993; Lin et al., 1994). Loss of *D*N-cadherin did not appear to perturb the pathfinding of the pioneers at stages 12 and 13, as the pioneer growth cones normally navigated and the vMP2 pathway was

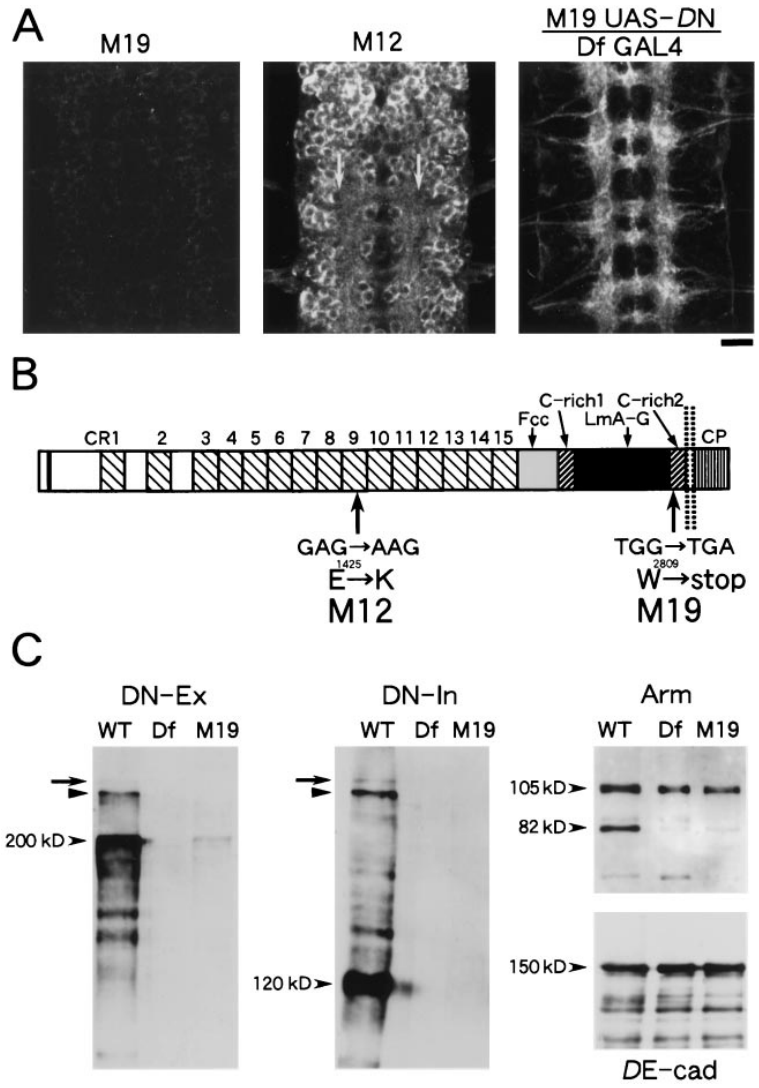

Figure 4. *D*N-cadherin is Encoded by *l(2)36Da*

(A) DN-Ex staining patterns of the CNS of *l(2)36Da* mutants at stage 14–15. (M19, left) Signals are hardly detectable in the CNS of homozygotes having a strong allele *l(2)36Da*^{M19}. (M12, middle) *D*N-cadherin is predominantly localized in neuronal cell bodies in the mutant with a weak allele *l(2)36Da*^{M12}. Arrows delineate the axon scaffold. The M19 image was adjusted to increase brightness strongly relative to the M12 picture so that the M19 tissue could be recognized; "signals" in M19 were due to nonspecific binding of a secondary antibody. (M19 UAS-*D*N/Df GAL4, right) Expression of *D*N-cadherin cDNA under UAS was driven by Sca-GAL4 in *l(2)36Da*^{M19} p[UAS-*D*N-cad]/*Df(2L) TW119* p[GAL4]. The cadherin molecules were abundant in axon tracts and midline cells, although the axonal signal was less intense than that in the wild-type embryo. Anterior is at the top, and the scale bar indicates 10 μm.

(B) *l(2)36Da*^{M19} and *l(2)36Da*^{M12} have nucleotide changes in the *D*N-cadherin gene. They result in either a nonsense mutation (M19) or a missense mutation (M12). Abbreviations and symbols are as explained in Figure 1A.

(C) Western analyses of mutant embryos. Extracts of the wild-type Oregon R (WT), homozygous *Df(2L)TW119* (Df), and homozygous *l(2)36Da*^{M19} embryos (M19) were analyzed for *D*N-cadherin, Arm, and *D*E-cadherin. Blots probed with DN-Ex and DN-In were overexposed. In M19, a faint signal of the 200 kDa fragment is seen, but neither the mature form (triangle) nor the 120 kDa fragment is detectable. Arrows mark positions of the precursor. Note that Df and M19 display preferential decreases in the level of the neuronal Arm isoform (82 kDa) in contrast to their normal expression of the ubiquitous form (105 kDa). In each lane, proteins equivalent to ~10 embryos (24–28 hr) were loaded onto the gels, and *D*E-cadherin (150 kDa) levels were similar.

generated as in the wild type (Figure 5A). Staining with another marker 22C10 (Fujita et al., 1982; Seeger et al., 1993) confirmed normal outgrowth of the vMP2 and MP1 axons at this stage. At stage 14 when follower neurons begin Fas II expression and join the pioneer tracts, three classes of pattern alteration were recognized (Figures 5B and 5C). First, in normal embryos, the vMP2 tract is constricted toward the midline in a segmentally repeated fashion, whereas the mutant route waved to a lesser extent. Moreover, local associations between the vMP2 and MP1 fascicles were diminished in the mutants. Second, one commissural axon fascicle periodically detected in each segment stained more intensely in the mutants than in the wild type (arrowhead in Figures 5B and 5C), implying that more axons joined the mutant fascicle. Third, the MP1 pathway sometimes looked discontinuous (1.6 breaks per embryo; n = 18), as marked with asterisks in Figure 5C. These results are illustrated in Figures 5D and 5E.

Irregular patterns became more conspicuous at late stage 16 when Fas II–positive axons were assembling into three longitudinal bundles (Figures 5F and 5G). Occasionally, the two more laterally located pathways were interrupted (3.4 breaks per embryo; n = 29), and the disconnected terminals were often swollen and/or had turned laterally (yellow arrows in Figure 5G). The bundles locally bifurcated (arrowheads in Figure 5G), which represents either defasciculation or abnormal fusion. Even when the bundles were not broken, the width of each path was more irregular than in the wild type, and the three longitudinal routes did not always run in parallel. The above phenotypes at late stages 14 and 16 make several explanations possible, such as reduced or altered interaction between fascicles, and stall or misorientation of growth cones. However, because of a number of Fas II–expressing follower axons, we could not obtain enough resolution to verify these possibilities.

Patterning of *apterous*-Expressing Axons Is Impaired in the Mutants

The LIM homeodomain transcription factor Apterous (Ap) is expressed in only three interneurons per abdominal hemisegment, and the fascicle of their ipsilaterally projecting axons can be monitored with a tau-lacZ transgene driven by an *ap* cis element (Lundgren et al., 1995). The *ap* axons first extend medially, then their

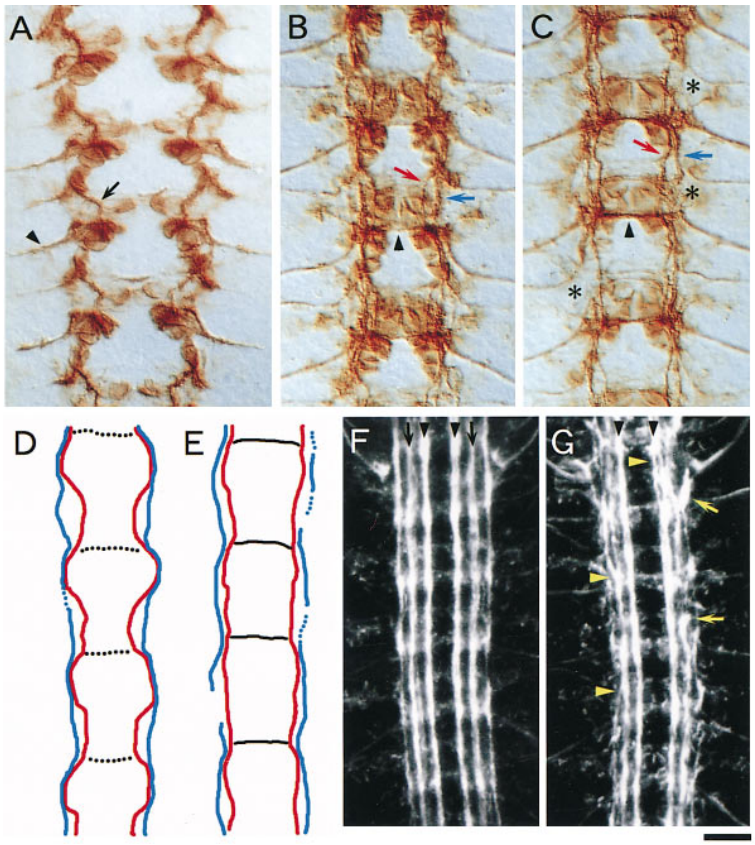

Figure 5. Aberrant Trajectories of Fasciclin II–Immunoreactive Fascicles in the Mutant Embryo

The wild-type and *l(2)36Da*^{M19}*/Df(2L)TW119* embryos were stained for fasciclin II.

(A) Stage 13 mutant embryo exhibits normal extension of pioneer pCC and aCC axons, indicated by the arrow and arrowhead, respectively.

(B and C) Late stage 14 embryos of the wild type (B) and the mutant (C). Red arrows point to the vMP2 fascicles; and blue ones, to the MP1 pathways. Arrowheads mark commissural axon bundles. Breaks in the MP1 pathways are indicated by asterisks.

(D and E) Axon fascicles in (B) and (C) were traced and depicted in (D) and (E), respectively. In the mutant (E), the vMP2 tracts (red) are deformed; and the MP1 tracts (blue) are locally disconnected. Black solid and broken lines indicate that the mutant formed thicker commissural fascicles than the wild type (D).

(F and G) Fas II–positive axon tracts in late stage 16 wild type (F) and mutant (G). Images of the entire Fas II axons were constructed by overlaying multiple confocal sections. At this stage, Fas II is expressed at high levels in three longitudinal bundles on each side. The most medial one (black arrowheads) is the MP1 fascicle, and more laterally located is the FN3 pathway (black arrows in [F]) (Lin et al., 1994). In (G), yellow arrows mark interruptions in the FN3 or in the most lateral fascicle, and yellow arrowheads indicate bipartite bundles.

Anterior is at the top. The scale bars indicate 13 μm in (A–E) and 10 μm in (F) and (G).

growth cones make right-angled turns and grow in an anterior direction (Figures 6A and 6C). Subsequently, the transverse portion of each *ap* axon starts a medial shift, and its turning point reaches the most medial surface of the longitudinal axon tracts (Figures 6A and 6E).

In the *D*N-cadherin mutant, the initial outgrowth and turning of the *ap* axons looked normal (Figure 6D). However, after the turn, the mutant fascicles took oblique trajectories in contrast to the parallel pathways in normal embryos (Figures 6F, 6H, and 6I). This pattern defect was due to impaired position shift of the transverse segments of the *ap* axons; in the mutants, their turning points remained at the original coordinates in the axon scaffold (yellow arrows in Figures 6F, 6H, and 6I). Nevertheless, the growth cone extended toward its canonical path, that is, the medial boundary of the longitudinal connectives. Consequently, the mutant axons drew arcs or ran obliquely. This angled extension was observed in 72% of 156 mutant abdominal hemisegments (A1–A7) at stage 16 and in only 2% of 211 wild-type hemisegments. We could rescue this phenotype at least in part by expressing *D*N-cadherin cDNA in the mutant nervous system by use of GAL4 driver strains, for example, panneural Sca-GAL4 (Klaes et al., 1994) (see Experimental Procedures). The Sca-GAL4-induced expression decreased the penetrance of the mutant phenotype to 15%. Similarly, the malformation of the Fas II fascicles was remedied by the cDNA expression in the mutants (data not shown).

Most of the mutant growth cones of the *ap* neurons reached adjacent anterior segments and navigated along the most medial path. However, they could not immediately fasciculate with the misrouted axons of counterpart neurons in those anterior segments. Besides the block of the medial shift, the mutants showed increased errors in axon bundling between ventral and dorsal *ap* cells (22% of 153 mutant hemisegments; Figure 7). The dorsal axon and the ventral axons sometimes failed to join (Figures 7B–7D); this failure of fasciculation was occasionally accompanied by misorientation of growth cones (Figure 7D). Such defective bundling as shown in Figures 7B–7D was rarely seen in the wild type (3% of 307 hemisegments). Without the fascicle formation, the mutant growth cones appeared to continue navigation (white arrows in Figure 6H), indicating that the bundling was not an absolute prerequisite for further axon outgrowth.

Except for the phenotypes described above, we did not detect obvious malformation in the central and peripheral nervous systems or in mesodermally derived tissues with the molecular markers employed. For example, fasciclin III– or *eagle*-positive axons extended contralaterally as in the wild type (Patel et al., 1987; Higashijima et al., 1996). No misrouting and defasciculation of motor and sensory axons was found by staining with Fas II and 22C10, respectively. Staining of mutants with anti-REPO showed normal glial patterns. Finally, generation of muscles and mesodermally derived glia (Edwards et al., 1993) was apparently unaffected, as shown by use of twist-lacZ as a marker (Thisse and Thisse, 1992).

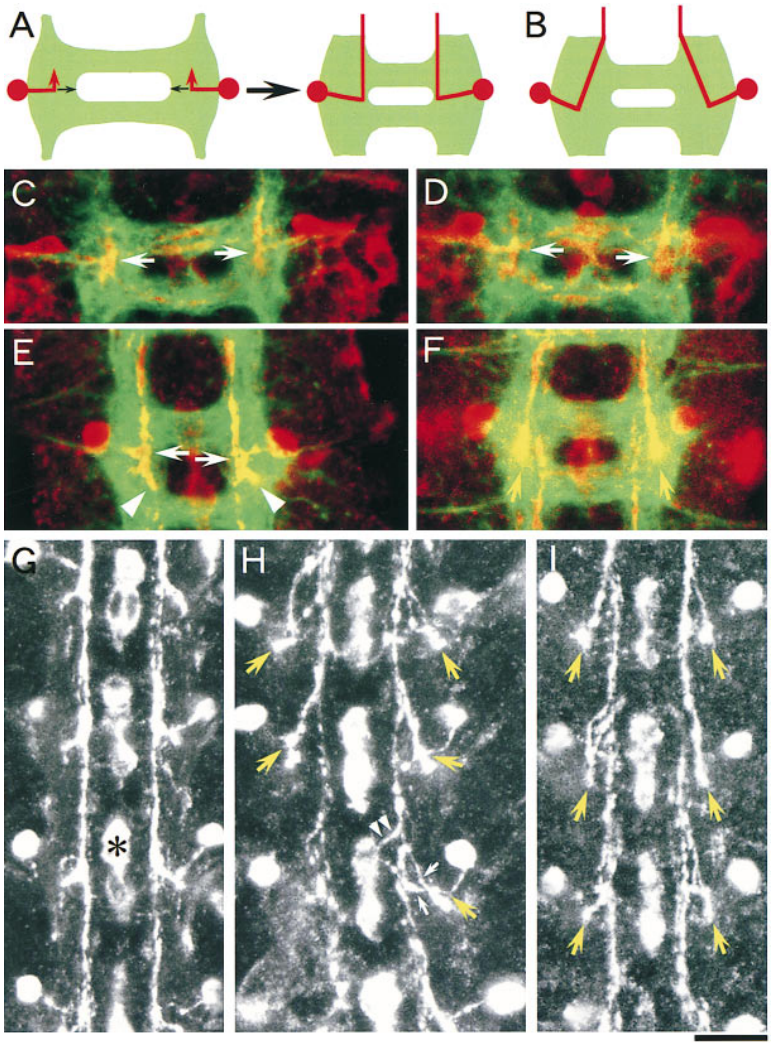

Figure 6. Transverse Portions of *apterous*-Expressing Neurons Do Not Shift Medially in the *D*N-cadherin Mutant

(A and B) Schematic illustration of early and late pathways of *apterous* (*ap*)-expressing neurons in the wild-type CNS (A), and aberrant tracts in a late-stage mutant *l(2)36Da*^{M19}/*Df(2L)TW119* (B). Each abdominal hemisegment has three *ap* neurons, one dorsal cell (red) and two ventrally positioned cells; and their axons fasciculate with each other. For simplicity, the ventral neurons are not drawn here. Whole CNS axon tracts are labeled in green. The small black arrows in (A) indicate medial position shifting of the *ap* axons.

(C–F) Merged images of the *ap* pathways (red) and entire CNS axons (green) in the wild type ([C] and [E]) and mutant ([D] and [F]).

(C and D) Stage 14 embryos.

(E and F) Stage 15–16 embryos. At stages 15–16, the *ap* longitudinal paths run along medial boundaries of the neuropil in the wild type (E). White arrows in (C–E) indicate turning points at normal positions. White arrowheads in (E) mark axons from ventral neurons whose cell bodies are out of the focal plane. In the mutant (F), the turning points did not move medially, but remained at lateral coordinates (yellow arrows), and axons ran obliquely. Out of the focal plane are axons between cell bodies of the dorsal neurons and the turning points; this is also the case in several segments in (G–I).

(G–I) Stage 16 embryos. Fascicles have already been connected to each other between segments in the wild type (G).

(H and I) Axon extensions from the mispositioned turning points (yellow arrows) displayed angled trajectories. In (H), small white arrows mark failure of association between ventral and dorsal axons, and double arrowheads point to local derailment of an axon. At stage 16, midline cells start the reporter expression (for example, asterisk in [G]). Anterior is at the top. The scale bar indicates 10 μm.

Discussion

*D*N-cadherin Is the Major Classic-Type Cadherin in Axons

We isolated a novel Drosophila cadherin, *D*N-cadherin. In the Drosophila cadherin superfamily, *D*N-cadherin is the first member that is broadly expressed in the nervous system and the mesoderm. Compared with the vertebrate classic cadherins, the *D*N-cadherin extracellular region is unusual with respect to its entire size, domain structures, and the number of cadherin repeats. Nevertheless, we provided three lines of evidence that *D*N-cadherin is homologous to vertebrate classic cadherins in the sense of local structure or molecular function: First, we found significant similarity in its intracellular sequences to those that are conserved among the identified classic cadherins. Second and most important, it formed a multiprotein complex with catenins. Third, we demonstrated homophilic cell binding activity. What distinguishes both *D*E- and *D*N-cadherins from the vertebrate molecules is a string of domains: Fcc box, C-rich region, and a laminin A globular domain. It remains to be investigated how crucial these domains are for functions of these molecules and whether such sequences are universal to the other cadherins in the arthropods or in other invertebrates.

Cadherin expression changes from the *D*E- to the *D*N-subclass during gastrulation and neurulation. These expression profiles are reminiscent of switching from E- to N-cadherin in equivalent morphogenetic events in vertebrate embryos (Hatta and Takeichi, 1986; Hatta et al., 1987; Dusband et al., 1988; Radice et al., 1997). Ectopic expression of N-cadherin in the Xenopus embryo induces various histological abnormalities, suggesting that precise quantitative and qualitative regulation of N-cadherin is essential for embryonic morphogenesis (Detrick et al., 1990; Fujimori et al., 1990). Significance of the switching pattern in Drosophila could be addressed also by misexpression experiments.

Recent studies on developing vertebrate brains show that a number of cadherin subclasses are expressed in spatially distinct manners (Suzuki et al., unpublished

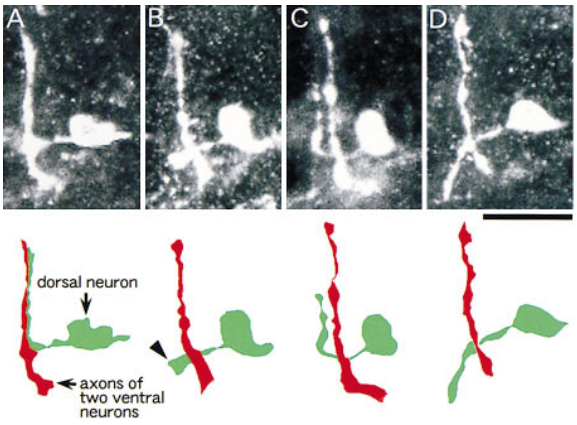

Figure 7. Ventral and Dorsal *ap* Axons Fail to Join Each Other in Some Mutant Hemisegments

(Top) Photographs of *ap* axons in stage 15 wild type (A) and *l(2)36Da*^{M19}*/Df(2L)TW119* mutants (B–D). Bottom panels are diagrams of our interpretation of individual top pictures. Normally, three axons, one from a dorsal cell (green) and two from ventral ones (red), are bundled (A), but this fasciculation is occasionally impaired in the mutants (B–D).

(B) The growth cone of the dorsal axon (arrowhead) has failed to join the ventral axons.

(C) The turning point of the dorsal axon has shifted medially as in the wild type, but those of the ventral axons did not.

(D) The growth cone of the dorsal axon has navigated in the wrong direction. Anterior is at the top. Medial is to the left. The axons of *ap* neurons are visualized with apC-tau-lacZ transgene (Lundgren et al., 1995), but anti-β-gal staining did not always give uniform signals along the axon. The scale bar indicates 10 μm.

data; reviewed by Redies, 1995; Redies and Takeichi, 1996). Strong down-regulation of catenins in *D*N-cadherin mutants suggests that *D*N-cadherin is the major classic-type cadherin expressed in axons, but this does not rule out the possibility that subsets of axon fascicles express other unidentified cadherins. In the course of cloning the *D*N-cadherin gene, we identified three other novel genes of the cadherin superfamily (see Experimental Procedures), and we are currently studying their expression patterns and molecular structures.

Processes of Axon Patterning That Critically Depend on *D*N-cadherin

The overall configuration of axon tracts was slightly distorted by the null mutation of the *D*N-cadherin gene. Aberrant patterns of axon trajectories were observable when we focused on the subsets of neurons that expressed either fasciclin II (Fas II; Lin et al., 1994) or *apterous* (*ap*; Lundgren et al., 1995). Initial axon elongation of Fas II–expressing pioneer neurons was unaffected, but outgrowth patterns became deformed after many follower axons joined the pioneer tracts. The *D*N-cadherin mutants at late stage 16 displayed discontinuous or derailed axon bundles, which suggest stall or misorientation of growth cones. Although verification of our interpretation awaits identification and labeling of a subpopulation, or ideally of a single cell, of the Fas II–positive follower neurons, the above phenotypes indicate that the pathfinding of the followers is regulated by cadherin-dependent contact with preexisting axons.

ap is expressed in only three neurons per abdominal hemisegment (Lundgren et al., 1995), and tracking of their migratory axons provided us insight into how loss of *D*N-cadherin influences axon patterning. In the *D*N-cadherin mutants, the most penetrant phenotype was that the *ap* axons could not carry out medial position shifting, suggesting an important role of this molecule in reorganization of axon fascicles. One possible explanation of this phenotype is as follows: In normal development, a group of medially located longitudinal axons initiates tight fascicle formation through *D*N-cadherin-mediated contacts. The *ap* axons, as soon as they finish turning and start anterior navigation, may be dragged into that bundling, which leads to the medial movement of the transverse segment of the *ap* axons. Hence, without *D*N-cadherin, the transverse segment would be left behind at a lateral position. Because of the broad neuronal distribution of *D*N-cadherin, we suppose that abnormal patterning is not restricted to the *ap* axons. If specific markers for other individual migratory fascicles become available, it would be possible to visualize more profound effects of *D*N-cadherin mutations on the overall neuronal architecture. Axons that are mispositioned in the mutant CNS may not be able to contact directly with correct partner axons; this would prevent development of interneuronal synapses that are generated between axons in the wild-type embryonic CNS (Tepass and Hartenstein, 1994). Previously, our group and another showed that in epithelia, zygotic *D*E-cadherin expression is required for cell rearrangement, one of the active morphogenetic processes (Tanaka-Matakatsu et al., 1996; Tepass et al., 1996; Uemura et al., 1996). Thus, the results of genetic analysis of both *D*N- and *D*E-cadherins emphasize that dynamic cellular reorganization critically depends on the action of the cadherin cell adhesion system.

It was demonstrated that *ap* function is required for controlling neuronal pathway selection of the *ap*-expressing cells; in 90% of segments of *ap* loss-of-function mutants, the *ap* neurons elongate their axons along inappropriate pathways, and these axons fail to fasciculate (Lundgren et al., 1995). Because Ap likely acts as a transcriptional regulator, it is speculated that Ap controls expression of cell surface receptors mediating specific recognition between the *ap* axons. Loss of ubiquitously expressed *D*N-cadherin also led to errors in fasciculation and directional guidance, although the penetrance was lower and the phenotypes were milder than those in the *ap* mutant. A similar case was found in Fas II–positive bundle formation. Absence of Fas II prevents the axons within the MP1 or the FN3 pathway from selectively adhering to one another, leading to dramatic defasciculation (Lin et al., 1994); in the *D*N-cadherin mutant, less severe phenotypes of altered fasciculation were observed. We take these results to indicate that cell type–specific recognition molecules make a primary contribution to selective fascicle formation and that generally present *D*N-cadherin facilitates the accomplishment of this formation with high fidelity. In generation and repatterning of individual fascicles, the extent of the phenotypes induced by the loss of *D*N-cadherin may not be disastrous in itself; however, such defects, if accumulated in various neuronal circuits, might result in the embryonic lethality.

Although *D*N-cadherin is broadly present at intercellular boundaries in the mesoderm besides in the nervous system, it is unlikely that the axonal phenotypes in the *D*N-cadherin mutant were secondary consequences of its depletion in the mesoderm. This is because there were no apparent morphological defects in mesodermal tissues and because the mutant phenotypes were rescued by *D*N-cadherin cDNA expression in the nervous system. Most likely, *D*N-cadherin plays a direct role in axon–axon interactions, as it is abundant in axons and not produced in glia except in those derived from the mesoderm.

Loss of *D*N-cadherin unmasked interesting longitudinal navigation of the growth cones of the *ap* neurons. When left behind at the lateral position, the *ap* growth cones steered toward the authentic, most medial pathway and migrated along it once they had reached that point. One hypothesis for this deflection would be that the growth cones responded to a chemoattractant either from the medial path or from the midline, and were directed in a *D*N-cadherin-independent manner. This speculative chemoattractant and its receptor could be, respectively, Drosophila netrins, whose expressions are elevated in the midline cells (Harris et al., 1996; Mitchell et al., 1996), and their putative receptor, Frazzled, which is widely localized in axon tracts (Kolodziej et al., 1996). The role of netrins in the outgrowth specifically of ipsilateral longitudinal axons such as the *ap* axons has not yet been examined.

Following pathfinding and target recognition, neurons form synapses to establish functional connections. In the vertebrates, developing synaptic contacts have abundant catenin-based junctions, which suggest a crucial function of the cadherin–catenin complex in the formation or maintenance of synaptic junctions (Fannon and Colman, 1996; Uchida et al., 1996). As interneuronal synapses are well characterized in the adult nervous system in Drosophila (Meinertzhagen and O'Neil, 1991; Hoshino et al., 1996; Sone et al., 1997), it will be interesting to explore the subcellular localization of *D*N-cadherin and catenins at the ultrastructural level in future studies.

Experimental Procedures

PCR and cDNA Cloning

The following primers were used to amplify cDNA of cadherin cytoplasmic regions (corresponding amino acid sequences are shown in parentheses):

CP1: 5′ GAATTCTA[T/C]GAIGAIGA[G/A]GG 3′ (YEDEG) CP2: 5′ GAA TTC[G/A]TACAT[G/A]TCIGCIA[G/A][T/C]TT 3′ (KLADMY) CP3: 5′ GAATTCA[T/C]TA[T/C]GCITA[T/C]GA[G/A]GG 3′ (HYAYEG) CP4: 5′ GAATTCAAIC[G/T]IGGICCCCA 3′ (WGPRF)

We amplified cDNA fragments of Bombyx cadherin-1, Bombyx cadherin-2, and *D*N-cadherin with primer combinations of CP1-CP2, CP3-CP2, and CP3-CP4, respectively. The template used in each PCR was a cDNA library from Bombyx embryos (made in Y. Suzuki's laboratory), Bombyx larval brains (made by M. Iwami), or Drosophila adult heads (made in L. and Y. N. Jans' laboratory). We sequenced 18 clones amplified with CP3 and CP4, and all were derived from the *D*N-cadherin gene. Then the head library was screened with these clones, and a 2.8 kb cDNA (AH2.8), which contained the entire intracellular domain of *D*N-cadherin, was isolated.

Fragments (150 bp) within extracellular cadherin repeats were amplified from a Drosophila embryo cDNA library (Zinn et al., 1988) with the following two primers:

Ex1: 5′ GATTCNNNN[T/C]TNGA[T/C][A/C]GNGA 3′ (XLDRE)
Ex2: 5′ GATTCNGGNNN[G/A]TT[G/A]TC[G/A]TT 3′ (NDNXP)

cDNA clones that hybridized with the 150 bp fragments were recovered from the same library. Subsequent cross-hybridization analyses showed that isolated clones were derived from at least six loci: *fat* (Mahoney et al., 1991), *dachsous* (Clark et al., 1995), and four novel genes. One clone of these novel genes, H4.5, gave expression patterns that were indistinguishable from those of AH2.8 in developmental Northern blots and embryonic RNA in situ hybridization. This strongly suggested that H4.5 included the extracellular portion of *D*N-cadherin, and, in fact, H4.5 contained the N-terminal 1349 amino acid residues. Reverse transcription (RT)–PCR amplified a cDNA clone, RT3.2, that connected H4.5 and AH2.8. Developmental Northern analysis showed the *D*N-cadherin transcript to be ~15 kb long and present most abundantly in embryos (data not shown).

We isolated 9.3 kb cDNA fragments that included the entire open reading frame by RT–PCR. Poly(A)$^+$ RNA was isolated from the wild-type OregonR embryos, and cDNA was made with Superscript (GIBCO-BRL). In this PCR, we employed Ex Taq DNA polymerase (Takara) and the following primers that have HindIII and NotI sites:

5′CCCAAGCTTGCGGCCGCAGTCAACAATTGAAGAGTGAGCACAT TGAAAAGGGA 3′
5′CCCAAGCTTGCGGCCGCTTACAATTCTAGTTCGGTATTGTGGG GATTGGGCGCCTC 3′

The 9.3 kb clones consisted of two classes of alternatively spliced products, and the alteration took place only within the seventh repeat (CR7 in Figure 1B and CR7′; the latter is not shown in this article). When S2 cells were transfected with these clones, two independent CR7 clones gave self-aggregating activity, but none of three CR7′ clones did. Western analyses showed that proteolytic maturation of precursors from all three CR7′ clones was partially blocked, as was the case with the product of *l(2)36Da*^{M12} (data not shown). Thus, we employed one of the CR7 clones, #6, in further experiments. Aside from sequences of the seventh cadherin repeat, clone #6 has five amino acid replacements when compared with the sequences of cDNA clones H4.5, RT3.2, and AH2.8. We do not know whether these substitutions are due to polymorphism or replication errors of Ex Taq polymerase. Amino acid sequences in Figure 1 are derived from those of H4.5, RT3.2, and AH2.8 except those in CR7.

Cell Culture and cDNA Transfection

For expression of *D*N-cadherin in S2 cells, an inducible expression plasmid was constructed as follows: A NotI site was created at the position of an EcoRI site of pRmHa3 (Bunch et al., 1988). Then the 9.3 kb CR7 clone #6 was inserted into this modified pRmHa3 (pRmHa3′). The resultant plasmid, pRmHa3′-DN, was transfected into S2 cells by the calcium phosphate precipitation method (Nagafuchi et al., 1987). Induction of cadherin expression in S2 cells and cell aggregation assay were as described previously (Oda et al., 1994) except that the cells were resuspended in Schneider's medium (GIBCO-BRL) supplemented with 10% fetal bovine serum. For preparation of Western samples, cells were further washed with saline. We attempted multiple times to isolate cell lines that stably expressed *D*N-cadherin by cotransfecting S2 cells with pPC4 (Jokerst et al., 1989) but could not establish such lines. In parallel experiments with pRmHa3-DECH (Oda et al., 1994), stable transfectants synthesizing *D*E-cadherin were reproducibly isolated.

Antibodies to Drosophila Cadherins and Catenins

To produce *D*N-cadherin fusion proteins in E. coli, we subcloned cDNA fragments that covered an extracellular portion (CR2–CR8) and the whole cytoplasmic domain into pGEX-1λT (Pharmacia) and pGEMEX-1 (Promega), respectively. Inclusion bodies of each fusion protein were prepared, mixed with RIBI adjuvant, and used to generate rat antisera and monoclonal antibodies. Monoclonal antibodies DN-Ex3, -Ex4, -Ex8, -Ex13, and -Ex14 recognized the extracellular region, whereas DN-In bound to the intracellular domain. Culture supernatants were used for subsequent experiments. Specificities of the antisera, DN-Ex and DN-IN, were verified by immunostaining

and/or Western blot analyses of homozygous *Df(2L)TW119* embryos. DN-In cross-reacted with an unknown molecule(s) at cell–cell boundaries in the epidermis, but only at embryonic stage 17. Western analyses and immunoprecipitation were done as described previously (Oda et al., 1993, 1994; Uemura et al., 1996), and *D*N-cadherin was detected in 5% polyacrylamide gel. Immunoprecipitation of *D*N-cadherin/catenin complexes (Figure 2) was performed with the antiserum to the intracellular domain. We previously characterized the rat antibodies to *D*E-cadherin (DCAD1 for Western analysis and DCAD2 for immunoprecipitation and immunohistochemistry) and *D*α-catenin (DCAT1) (Oda et al., 1993, 1994).

Drosophila Strains

Deficiency chromosomes and essential loci in the 36A–36F region were previously reported (Steward and Nüsslein-Volhard, 1986). Embryos were collected from various deficiency strains and stained with *D*N-cad antibodies. This analysis placed the gene between the distal break point of *Df(2L)MHS5* and that of *Df(2L)TW201*. In this interval, *l(2)Bld* is the only known locus that is essential for viability (Steward and Nüsslein-Volhard, 1986). *l(2)Bld*, which was shown to encode *D*N-cadherin in this study, was renamed *l(2)36Da* (Lindsley and Zimm, 1992). Alleles of five strong loss-of-function mutations were designated as M6, M19, M23, M33, and F15; and one hypomorph was named M12. Some of the *l(2)36Da* chromosomes appear to have mutations outside *Df(2L)TW119*, which affected CNS morphogenesis. Therefore, we studied embryonic phenotypes of each *l(2)36Da* allele over *Df(2L)TW119*. Removal of the *D*N-cadherin gene in the *Df(2L)TW119* chromosome was verified by probing its genomic DNA with the cDNA clones. To distinguish mutant embryos and larvae from heterozygous ones, we balanced *l(2)36Da* and *Df(2L)TW119* chromosomes with *CyO* p[y+] or *CyO* p[ftz-lacZ] (Hiromi et al., 1985). In experiments of Figures 4B and 4C, *yw*; *l(2)36Da*/*CyO* p[y+] and *yw*; *Df(2L)TW119*/*CyO* p[y+] were employed, and mutant embryos (y^-) were sorted for RNA extraction or for the Western analysis.

Three transgene markers were used to characterize *D*N-cadherin mutants: apC-tau-lacZ 2.1 (an insertion on the third chromosome; Lundgren et al., 1995), eagle-kinesin-lacZ K42 (the third chromosome; Higashijima et al., 1996), and twist-lacZ (the second chromosome; Thisse and Thisse, 1992). As for the third chromosome transgenes, mutant embryos were collected from crosses of *Df(2L)TW119*/+; transgene/+ and $l(2)36Da^{M19}$/+; transgene/+, and doubly labeled with DN-Ex and anti-β-gal. The wild-type control embryos were collected from crosses of heterozygotes (transgene/+). We collected images of the wild-type or mutant embryos with two copies of apC-tau-lacZ. Ectopic expression of *glial cell missing* was done as described by Hosoya et al. (1995). A transformation construct p[UAS-*D*N-cad] is a pUAST derivative, which has the 9.3 kb *D*N-cadherin cDNA. Recovery of phenotypes was investigated in embryos of $l(2)36Da^{M19}$ p[UAS-*D*N-cad]/*Df(2L) TW119* p[GAL4]. Employed GAL4 driver strains were Scabrous-GAL4 (Klaes et al., 1994) and GAL4-1407 (Luo et al., 1994).

Sequence Analyses of *l(2)36Da* Alleles

Poly(A)$^+$ RNA was recovered from $l(2)36Da^{M12}$/*Df(2L)TW119* adults or $l(2)36Da^{M19}$ homozygous embryos by use of a QuickPrep Micro mRNA Purification Kit (Pharmacia Biotech). First strands of cDNA were made with Ready-To-Go Beads (Pharmacia Biotech) and directly used for PCR amplification of mutant *D*N-cadherin cDNA with Pfu polymerase (Stratagene). To cover the entire open reading frame, we employed 11 primer pairs; individual primer sets were designed to amplify 0.8–1.3 kb cDNA. Mutant sequences of both strands were determined by use of fluorescently labeled primers and electrophoresis in a DNA sequencer (Aroka). Base substitutions in the mutants were confirmed in multiple cDNA clones amplified with two different pairs of primers.

Observation of Embryos

Procedures for immunostaining were essentially as described (Oda et al., 1994; Uemura et al., 1996). Antibodies used were as follows: 7A1 (mouse anti-Arm; Peifer, 1993), 1D4 (mouse anti-fasciclin II; Van Vactor et al., 1993), BP102 (Seeger et al., 1993), rabbit anti-REPO (Halter et al., 1995), 7G10 (mouse anti-fasciclin III; Patel et al., 1987), 22C10 (Fujita et al., 1982), anti-HRP (Jan and Jan, 1982; Cappel), and rabbit anti-β-galactosidase (Cappel). Signals were detected by peroxidase reactions visualized with an ABC Elite kit (Vectastain) or by fluorescence labeling. A combination of FITC and TexasRed was usually employed for double labeling, and embryos were viewed with a Zeiss or Biorad laser scanning confocal microscope. For detection of apC-tau-lacZ (Lundgren et al., 1995), fixed embryos were incubated with the anti-β-galactosidase, biotinylated anti-rabbit IgG (Amersham), and finally Cy3-conjugated streptavidin (Jackson).

Acknowledgments

The authors would like to thank M. Bate, S. Hayashi, T. Hosoya, Y. Hotta, T. Isshiki, L. Luo, A. Nose, B. Thisse, and especially J. Thomas for strains; M. Peifer, G. Technau, and in particular C. Goodman for antibodies; M. Iwami, H. Kokubo, K. Ohno, and Y. Suzuki for Bombyx cDNA libraries; and H. Ohkura for a cosmid clone that hybridizes with the *D*N-cadherin cDNA. We are grateful to M. Murata, S. Saito, and M. Yanagida for giving us opportunities to use their confocal microscopes; and members of A. Nose's group for allowing us to perform microinjection in their laboratory. We acknowledge the Human Genome Center at the Institute of Medical Sciences of Tokyo University for use of its databases. Finally, we thank A. Nose and J. Thomas very much for critical comments about our manuscript. This work was supported by a Grant-in-Aid for Creative Fundamental Research from the Ministry of Education, Science, and Culture of Japan to M. T.; T. U. is a recipient of a Fellowship of the Japan Society for the Promotion of Science for Junior Scientists.

Received May 2, 1997; revised May 27, 1997.

References

Bixby, J.L., and Zhang, R. (1990). Purified N-cadherin is a potent substrate for the rapid induction of neurite outgrowth. J. Cell Biol. *110*, 1253–1260.

Brand, A.H., and Perrimon, N. (1993). Targeted gene expression as a means of altering cell fates and generating dominant phenotypes. Development *118*, 401–415.

Bunch, T.A., Grinblat, Y., and Goldstein, L.S.B. (1988). Characterization and use of the Drosophila metallothionein promotor in cultured Drosophila melanogaster cells. Nucleic Acids Res. *16*, 1043–1061.

Campbell, G., Goring, H., Lin, T., Spana, E., Anderson, S., Doe, C.Q., and Tomlinson, A. (1994). RK2, a glial-specific homeodomain protein required for embryonic nerve cord condensation and viability in Drosophila. Development *120*, 2957–2966.

Chan, S.S.-Y., Zheng, H., Su, M.-W., Wilk, R., Killeen, M.T., Hedgecock, E.M., and Culotti, J.G. (1996). UNC-40, a C. elegans homolog of DCC (deleted in colorectal cancer), is required in motile cells responding to UNC-6 netrin cues. Cell *87*, 187–195.

Clark, H.F., Brentrup, D., Schneitz, K., Bieber, A., Goodman, C., and Noll, M. (1995). Dachsous encodes a member of the cadherin superfamily that controls imaginal disc morphogenesis in Drosophila. Genes Dev. *9*, 1530–1542.

Cox, R.T., Kirkpatrick, C., and Peifer, M. (1996). Armadillo is required for adherens junction assembly, cell polarity, and morphogenesis during Drosophila embryogenesis. J. Cell Biol. *134*, 133–148.

Detrick, R.J., Dickey, D., and Kintner, C. (1990). The effects of N-cadherin misexpression on morphogenesis in Xenopus embryos. Neuron *4*, 493–506.

Doherty, P., and Walsh, F.S. (1996). CAM-FGF receptor interactions: a model for axonal growth. Mol. Cell. Neurosci. *8*, 99–111.

Dusband, J.-L., Volberg, T., Sabanay, I., Thiery, J.-P., and Geiger, B. (1988). Spatial and temporal distribution of the adherens-junction-associated adhesion molecule A-CAM during avian embryogenesis. Development *103*, 325–344.

Edwards, J.S., Swales, L.S., and Bate, M. (1993). The differentiation between neuroglia and connective tissue sheath in insect ganglia revisited: the neural lamella and perineurial sheath cells are absent

in a mesodermless mutant of Drosophila. J. Comp. Neurol. *333*, 301–308.

Fannon, A.M., and Colman, D.R. (1996). A model for central synaptic junctional complex formation based on the differential adhesive specificities of the cadherins. Neuron *17*, 423–434.

Fujimori, T., Miyatani, S., and Takeichi, M. (1990). Ectopic expression of N-cadherin perturb histogenesis in Xenopus embryos. Development *110*, 97–104.

Fujita, S.C., Zipursky, S.L., Benzer, S., Ferrus, A., and Shotwell, S.L. (1982). Monoclonal antibodies against the Drosophila nervous system. Proc. Natl. Acad. Sci. USA *79*, 7929–7933.

Goodman, C.S. (1996). Mechanisms and molecules that control growth cone guidance. Annu. Rev. Neurosci. *19*, 341–377.

Goodman, C.S., and Doe, C.Q. (1993). Embryonic development of the Drosophila central nervous system. In The Development of Drosophila melanogaster, M. Bate and A. M. Arias, eds. (Cold Spring Harbor, New York: Cold Spring Harbor Laboratory Press), pp. 1131–1206.

Grenningloh, G., Rehm, E.J., and Goodman, C.S. (1991). Genetic analysis of growth cone guidance in Drosophila: fasciclin II functions as a neuronal recognition molecule. Cell *67*, 45–57.

Halter, D.A., Urban, J., Rickert, C., Ner, S.S., Ito, K., Travers, A.A., and Technau, G.M. (1995). The homeobox gene *repo* is required for the differentiation and maintenance of glia function in the embryonic nervous system of Drosophila melanogaster. Development *121*, 317–332.

Hammond, C., and Helenius, A. (1994). Quality control in the secretory pathway: retention of a misfolded viral membrane glycoprotein involves cycling between the ER, intermediate compartment, and Golgi apparatus. J. Cell Biol. *126*, 41–52.

Harris, R., Sabatelli, L.M., and Seeger, M.A. (1996). Guidance cues at the Drosophila CNS midline: identification and characterization of two Drosophila netrin/UNC-6 homolog. Neuron *17*, 217–228.

Hatta, K., and Takeichi, M. (1986). Expression of N-cadherin adhesion molecules associated with early morphogenetic events in chick development. Nature *320*, 447–449.

Hatta, K., Takagi, S., Fujisawa, H., and Takeichi, M. (1987). Spatial and temporal expression pattern of N-cadherin cell adhesion molecules correlated with morphogenetic processes of chicken embryos. Dev. Biol. *120*, 215–227.

Higashijima, S., Shishido, E., Matsuzaki, M., and Saigo, K. (1996). *eagle*, a member of the steroid receptor gene superfamily, is expressed in a subset of neuroblasts and regulates the fate of their putative progeny in the Drosophila CNS. Development *122*, 527–536.

Hirano, S., Kimoto, N., Shimoyama, Y., Hirohashi, S., and Takeichi, M. (1992). Identification of a neural α-catenin as a key regulator of cadherin function and multicellular organization. Cell *70*, 293–301.

Hiromi, Y., Kuroiwa, A., and Gehring, W.J. (1985). Control elements of the Drosophila segmentation gene *fushi tarazu*. Cell *43*, 603–613.

Hoshino, M., Suzuki, E., Nabeshima, Y.-I., and Hama, C. (1996). Hikaru genki protein is secreted into synaptic clefts from an early stage of synapse formation in Drosophila. Development *122*, 589–597.

Hosoya, T., Takizawa, K., Nitta, K., and Hotta, Y. (1995). *glial cells missing*: a binary switch between neuronal and glial determination in Drosophila. Cell *82*, 1025–1036.

Huber, O., Bierkamp, C., and Kemler, R. (1996). Cadherins and catenins in development. Curr. Opin. Cell Biol. *8*, 685–691.

Jan, L.Y., and Jan, Y.N. (1982). Antibodies to horseradish peroxidase as specific neuronal markers in Drosophila and grasshopper embryos. Proc. Natl. Acad. Sci. USA *79*, 2700–2704.

Jan, Y.N., and Jan, L.Y. (1993). The peripheral nervous system. In The Development of Drosophila melanogaster, M. Bate and A.M. Arias, eds. (Cold Spring Harbor, New York: Cold Spring Harbor Laboratory Press), pp. 1207–1244.

Jokerst, R.S., Weeks, J.R., Zehring, W.A., and Greenleaf, A.L. (1989). Analysis of the gene encoding the largest subunit of RNA polymerase II in Drosophila. Mol. Gen. Genet. *215*, 266–275.

Jones, B.W., Fetter, R.D., Tear, G., and Goodman, C.S. (1995). *glial cells missing*: a genetic switch that controls glial versus neuronal fate. Cell *82*, 1013–1023.

Kawanishi, J., Kato, J., Sasaki, K., Fujii, S., Watanabe, N., and Niitsu, Y. (1994). Loss of E-cadherin-dependent cell–cell adhesion due to mutation of the β-catenin gene in a human cancer cell line, HSC-39. Mol. Cell. Biol. *15*, 1175–1181.

Keino-Masu, K., Masu, M., Hinck, L., Leonardo, E.D., and Tessier-Lavigne, M. (1996). Deleted in colorectal cancer (DCC) encodes a netrin receptor. Cell *87*, 175–185.

Keynes, R., and Cook, M.W.G. (1995). Axon guidance molecules. Cell *83*, 161–169.

Klaes, A., Menne, T., Stollewerk, A., Schoiz, H., and Klämbt, C. (1994). The Ets transcription factors encoded by the Drosophila gene *pointed* direct glial cell differentiation in the embryonic CNS. Cell *78*, 149–160.

Kolodziej, P.A., Timpe, L.C., Mitchell, K.J., Fried, S.R., Goodman, C.S., Jan, L.Y., and Jan, Y.N. (1996). *frazzled* encodes a Drosophila member of the DCC immunoglobulin subfamily and is required for CNS and motor axon guidance. Cell *87*, 197–204.

Lin, D.M., Fetter, R.D., Kopczynski, C., Grenningloh, G., and Goodman, C.S. (1994). Genetic analysis of fasciclin II in Drosophila: defasciculation, refasciculation, and altered fasciculation. Neuron *13*, 1055–1069.

Lindsley, D.L., and Zimm, G.G. (1992). The Genome of Drosophila melanogaster. (New York: Academic Press, Inc.).

Lundgren, S.E., Callahan, C.A., Thor, S., and Thomas, J.B. (1995). Control of neuronal pathway selection by the Drosophila LIM homeodomain gene *apterous*. Development *121*, 1769–1773.

Luo, L., Liao, Y.J., Jan, L.Y., and Jan, Y.N. (1994). Distinct morphogenetic functions of similar small GTPases: Drosophila Drac1 is involved in axonal outgrowth and myoblast fusion. Genes Dev. *8*, 1787–1802.

Mahoney, P.A., Weber, U., Onofrechuk, P., Biessmann, H., Bryant, P.J., and Goodman, C.S. (1991). The *fat* tumor suppressor gene in Drosophila encodes a novel member of the cadherin gene superfamily. Cell *67*, 853–868.

Matsunaga, M., Hatta, K., Nagafuchi, A., and Takeichi, M. (1988). Guidance of optic nerve fibers by N-cadherin adhesion molecules. Nature *334*, 62–64.

Matsunami, H., and Takeichi, M. (1995). Fetal brain subdivisions defined by R-and E-cadherin expressions: evidence for the role of cadherin activity in region-specific, cell–cell adhesion. Dev. Biol. *172*, 466–478.

McCrea, P.D., Turck, C.W., and Gumbiner, B. (1991). A homolog of the armadillo protein in Drosophila (Plakoglobin) associated with E-cadherin. Science *254*, 1359–1361.

Meinertzhagen, I.A., and O'Neil, S.D. (1991). Synaptic organization of columnar elements in the lamina of the wild type in Drosophila melanogaster. J. Comp. Neurol. *305*, 232–263.

Mitchell, K.J., Doyle, J.L., Serafini, T., Kennedy, T.E., Tessier-Lavigne, M., Goodman, C.S., and Dickson, B.J. (1996). Genetic analysis of netrin genes in Drosophila: netrins guide CNS commissural axons and peripheral motor axons. Neuron *17*, 203–215.

Miyatani, S., Shimamura, K., Hatta, M., Nagafuchi, A., Nose, A., Matsunaga, M., Hatta, K., and Takeichi, M. (1989). Neural cadherin: role in selective cell–cell adhesion. Science *245*, 631–635.

Nagafuchi, A., Shirayoshi, Y., Okazaki, K., Yasuda, K., and Takeichi, M. (1987). Transformation of cell adhesion properties by exogenously introduced E-cadherin cDNA. Nature *329*, 341–343.

Nagafuchi, A., Takeichi, M., and Tsukita, S. (1991). The 102 kd cadherin-associated protein: similarity to vinculin and posttranscriptional regulation of expression. Cell *65*, 849–857.

Nagafuchi, A., Ishihara, S., and Tsukita, S. (1994). The roles of catenins in the cadherin-mediated cell adhesion: functional analysis of E-cadherin–α catenin fusion molecules. J. Cell Biol. *127*, 235–245.

Nagar, B., Overduin, M., Ikura, M., and Rini, J.M. (1996). Structural basis of calcium-induced E-cadherin rigidification and dimerization. Nature *380*, 360–364.

Oda, H., Uemura, T., Shiomi, K., Nagafuchi, A., Tsukita, S., and

Takeichi, M. (1993). Identification of a Drosophila homologue of α-catenin and its association with the armadillo protein. J. Cell Biol. *121*, 1133–1140.

Oda, H., Uemura, T., Harada, Y., Iwai, Y., and Takeichi, M. (1994). A Drosophila homolog of cadherin associated with Armadillo and essential for embryonic cell–cell adhesion. Dev. Biol. *165*, 716–726.

O'Kane, C., and Gehring, W. (1987). Detection in situ of genomic regulatory elements in Drosophila. Proc. Natl. Acad. Sci. USA *84*, 9123–9127.

Oyama, T., Kanai, Y., Ochiai, A., Akimoto, S., Oda, T., Yanagihara, T., Nagafuchi, A., Tsukita, S., Shibamoto, S., Ito, F., Takeichi, M., Matsuda, H., and Hirohashi, S. (1995). A truncated β-catenin disrupts the interaction between E-cadherin and α-catenin: a cause of loss of intercellular adhesiveness in human cancer cell lines. Cancer Res. *54*, 6282–6287.

Pai, L.-M., Kirkpatrick, C., Blanton, J., Oda, H., Takeichi, M., and Peifer, M. (1996). Drosophila α-catenin and E-cadherin bind to distinct regions of Drosophila Armadillo. J. Biol. Chem. *271*, 32411–32420.

Patel, N.H., Snow, P.M., and Goodman, C.S. (1987). Characterization and cloning of fasciclin III: a glycoprotein expressed on a subset of neurons and axon pathways in Drosophila. Cell *48*, 975–988.

Pearson, W.R., and Lipman, D.J. (1988). Improved tools for biological sequence comparison. Proc. Nat. Acad. Sci. USA *85*, 2444–2448.

Peifer, M. (1993). The product of the Drosophila segment polarity gene *armadillo* is part of a multi-protein complex resembling the vertebrate adherens junction. J. Cell Sci. *105*, 993–1000.

Radice, G.L., Rayburn, H., Matsunami, H., Knudsen, K.A., Takeichi, M., and Hynes, R.O. (1997). Developmental defects in mouse embryos lacking N-cadherin. Dev. Biol. *181*, 64–78.

Ranscht, B. (1994). Cadherins and catenins: interactions and functions in embryonic development. Curr. Opin. Cell Biol. *6*, 740–746.

Redies, C. (1995). Cadherin expression in the developing vertebrate CNS: from neuromeres to brain nuclei and neural circuits. Exp. Cell Res. *220*, 243–256.

Redies, C., and Takeichi, M. (1996). Cadherins in the developing central nervous system: an adhesive code for segmental and functional subdivisions. Dev. Biol. *180*, 413–423.

Riehl, R., Johnson, K., Bradley, R., Grunwald, G.B., Cornel, E., Lifenbaum, A., and Holt, C.E. (1996). Cadherin function is required for axon outgrowth in retinal ganglion cells in vivo. Neuron *17*, 837–848.

Sasaki, M., Kleinman, H.K., Huber, H., Deutzmann, R., and Yamada, Y. (1988). Laminin, a multidomain protein. The A chain has a unique globular domain and homology with the basement membrane proteoglycan and the laminin B chains. J. Biol. Chem. *263*, 16536–16544.

Schneider, T., Reiter, C., Eule, E., Bader, B., Lichte, B., Nie, Z., Schimansky, T., Ramos, R.G.P., and Fischbach, K.-F. (1995). Restricted expression of the irreC-rst protein is required for normal axonal projections of columnar visual neurons. Neuron *15*, 259–271.

Seeger, M., Tear, G., Ferres-Marco, D., and Goodman, C.S. (1993). Mutations affecting growth cone guidance in Drosophila: genes necessary for guidance toward or away from the midline. Neuron *10*, 409–426.

Shapiro, I., Fannon, A.M., Kwong, P.D., Thompson, A., Lehmann, M.S., Grubel, G., Legrand, J.F., Als-Nielsen, J., Colman, D.R., and Hendrickson, W.A. (1995). Structural basis of cell–cell adhesion by cadherins. Nature *374*, 327.

Sone, M., Hoshino, M., Suzuki, E., Kuroda, S., Kaibuchi, K., Kakagoshi, H., Saigo, K., Nabeshima, Y.-I., and Hama, C. (1997). Still life, a protein in synaptic terminals of Drosophila homologous to GDP–GTP exchangers. Science *275*, 543–547.

Spradling, A.C., Stern, D.M., Kiss, I., Roote, J., Laverty, T., and Rubin, G.M. (1995). Gene disruptions using P transposable elements: an integral component of the Drosophila genome project. Proc. Natl. Acad. Sci. USA *92*, 10824–10830.

Steward, R., and Nüsslein-Volhard, C. (1986). The genetics of the *dorsal-bicaudal-D* region of Drosophila melanogaster. Genetics *113*, 665–678.

Takeichi, M. (1991). Cadherin cell adhesion receptors as a morphogenetic regulator. Science *251*, 1451–1455.

Takeichi, M. (1995). Morphogenetic roles of classic cadherins. Curr. Opin. Cell Biol. *7*, 619–627.

Tanaka-Matakatsu, M., Uemura, T., Oda, H., Takeichi, M., and Hayashi, S. (1996). Cadherin-mediated cell adhesion and cell motility in Drosophila trachea regulated by the transcription factor Escargot. Development *122*, 3697–3705.

Tepass, U., and Hartenstein, V. (1994). The development of cellular junctions in the Drosophila embryo. Dev. Biol. *161*, 563–596.

Tepass, U., Gruszynski-DeFeo, E., Haag, T.A., Omatyar, L., Torok, T., and Hartenstein, V. (1996). *shotgun* encodes Drosophila E-cadherin and is preferentially required during cell rearrangement in the neuroectoderm and other morphogenetically active epithelia. Genes Dev. *10*, 672–685.

Tessier-Lavigne, M., and Goodman, C.S. (1996). The molecular biology of axon guidance. Science *274*, 1123–1133.

Thisse, C., and Thisse, B. (1992). Dorsoventral development of the Drosophila embryo is controlled by a cascade of transcriptional regulators. Dev. Suppl. 173–181.

Uchida, N., Honjo, Y., Jonson, K.R., Wheelock, M., and Takeichi, M. (1996). The catenin/cadherin adhesion system is localized in synaptic junctions bordering transmitter release zones. J. Cell Biol. *135*, 767–779.

Uemura, T., Oda, H., Kraut, R., Hayashi, S., Kataoka, Y., and Takeichi, M. (1996). Zygotic Drosophila E-cadherin expression is required for processes of dynamic epithelial cell rearrangement in the Drosophila embryo. Genes Dev. *10*, 659–671.

Ushkaryov, Y.A., Petrenko, A.G., Geppert, M., and Südhof, T.C. (1992). Neurexins: synaptic cell surface proteins related to the α-latrotoxin receptor and laminin. Science *257*, 50–56.

Van Vactor, D., Sink, H., Fambrough, D., Tsoo, R., and Goodman, C.S. (1993). Genes that control neuromuscular specificity in Drosophila. Cell *73*, 1137–1153.

Xiong, W.-C., Okano, H., Patel, N.H., Blendy, J.A., and Montell, C. (1994). *repo* encodes a glial-specific homeo domain protein required in the Drosophila nervous system. Genes Dev. *8*, 981–994.

Zinn, K., McAllister, L., and Goodman, C.S. (1988). Sequence analysis and neuronal expression of fasciclin I in grasshopper and Drosophila. Cell. *53*, 577–587.

GenBank Accession Numbers

The nucleotide sequence data reported in this paper will appear in the DDBJ, EMBL, and GenBank nucleotide sequence databases with the following accession numbers: AB002395 (Bombyx cadherin-1), AB002396 (Bombyx cadherin-2), and AB002397 (*D*N-cadherin). FASTA was used to search databases (Pearson and Lipman, 1988).

Note Added in Proof

Not only the *D*N-cadherin mutant, but also *armadillo* mutants have defects in axon fasciculation (Loureiro and Peifer, personal communication). The article cited as Suzuki et al., unpublished data, is now in press: Suzuki, S.C., Inoue, T., Kimura, Y., Tanaka, T., and Takeichi, M. (1997). Neuronal circuits are subdivided by differential expression of type-II classic cadherins in postnatal mouse brains. Mol. Cell. Neurosci., in press.